PROCEEDINGS REPRINT

SPIE–The International Society for Optical Engineering

Reprinted from

Smart Structures and Materials 1994

Smart Sensing, Processing, and Instrumentation

14–16 February 1994
Orlando, Florida

SPIE P PROCEEDINGS SERIES

Volume 2191

R-36615

1871

Dissipated energy as the means for health monitoring of smart structures

6383

Phillip W. Mast, John G. Michopoulos,
Robert Badaliance, Henry Chaskelis

Materials Science and Technology Division
Mechanics of Materials Branch, Code 6380
Naval Research Laboratory
Washington DC

ABSTRACT

NRL's Mechanics of Materials Branch has developed a technology that facilitates sensor selection and placement within a composite structure. The Embedded Sensors for Smart Structures Simulator (ES^4) is a design tool that relates the output of a finite number of sensors t strain induced structural damage. This tool is based on the use of the dissipative part of the bulk nonlinear material behavior. The methodolog used to identify this behavior has evolved at NRL over the past 20 years.

This paper describes the role of strain measurements and their relation to sensor type and location, the conceptual framework of dissipate energy density as the metric employed for assessing material/structure performance, the facilities provided by the simulator and their use, a well as implementation details.

Through this we hope not only to make designing and verifying embedded sensor layouts on composite material structures a tractable task, but also to promote the use of dissipated energy density as a foundation upon which to built an effective means of measuring material and structural health.

1. INTRODUCTION

1.1. Background

Current research on "Smart" or "Active" materials and structures, in most cases, associates material and structural health with strains c a derivative quantity. In this paper we promote the use of Dissipated Energy Density as a necessary argument to any material/structure healt function, and we also promote the use of the ES^4 tool to establish the required number of sensors, their type and placement, as well as materi and structural health monitoring schemes.

1.2. Assumptions

The method for the derivation and the usage of dissipated energy density function for a material system makes the following assumptior

- The composite material system used for the structure has been identified according to NRL's method of extracting the nonlinear materi behavior of the system, as captured in the form of the dissipated energy density function [1].
- Sensor transfer functions (forward and inverse), and calibration data are available.
- The structural loading rates lie within a range over which the dissipated energy density function for the material is deemed constant fc a given loading level.
- The loading condition applied on the structure at any instance, can be always reconstructed as a linear combination of a given and pe haps large set of basis loading cases.

Some of these assumptions affect the use of dissipated energy density based methodology for assessing health, and some affect the pr cess of evaluating the global strain field from the sensor outputs.

The method has been applied so far only to organic matrix composites.

1.3. Goals and Objectives

The overall strategy followed was motivated by a need to perform the following activities:

- Sensor Network Selection: The selection of sensor type and layout topology.
- Sensor Network Calibration: The calibration of installed sensors.
- Loading Event Simulation: Providing a capability to predict equivalent structural loading from sensor outputs.

Realization of these goals, involves resolving a number of technical issues.

1.4. Technical Issues

Associated with the sensor utilization scheme are these "how to" issues:
- utilize apriori material and structural knowledge
- provide fault tolerance and economic redundancy
- provide independence from structural size and shape considerations
- predict the material state in areas remote from sensor locations
- select an appropriate measure of "Health" which can be defined in terms of sensor output and which provides a spatially and temporally continuous assessment of material state that reflects the degree of material damage
- real time computation capability with reasonable computing resources

To address these issues we have developed an approach that first reconstructs the global structural strain field from the sensor network outputs and from that strain field then predicts the local and global structural health.

2. APPROACH

2.1. Computation of Sensor Predicted Strains

We assume that the geometric model of the structure can be covered by a mesh of n nodal points as shown in Figure 1.
The applied loading at any given moment can be considered a linear combination of r basis loading cases. Figure 1 shows the structure under the influence of the bth basis loading case, where the vertical line signifies the amplitude of strain component u at nodal point i.
The strain field corresponding to the bth basis loading case, L_b is represented by $\varepsilon_{ui}(L_b)$. Where u is the index for strain components and i is the index for the nodal point.and their ranges are given by:

$$\begin{aligned} i &\in \{1, \ldots, n\} \\ u &\in \{1, 2, 3\} \\ b &\in \{1, \ldots, r\} \end{aligned} \tag{1}$$

The strain field induced by an arbitrary loading situation, ε_{ui}, can then be thought of as that resulting from a linear combination of the basis strain fields, $\varepsilon_{ui}(L_b)$, associated with each one of the basis loadings L_b, according to:

$$e_{ui} = \varepsilon_{ui}(L_b)\,\alpha_b. \tag{2}$$

Where α_b are the proportions contributed by individual basis strain fields, $\varepsilon_{ui}(L_b)$.

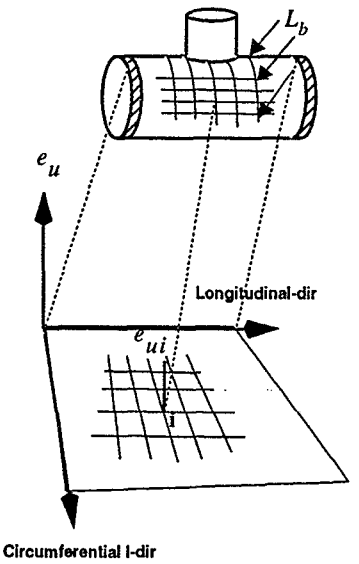

Fig. 1. Strain space associated with the geometry of the structure.

The basis strain fields $\varepsilon_{ui}(L_b)$ can be computed once via linear elastic finite element analyses and stored for future use. The strains given by equation (2) are the ones that the structure will experience when the corresponding loading is applied to the structure. It is expected that for the general case where grossly asymmetrical sensitivity and/or closeness between basis strain cases exist, the basis will be conditioned by projection into to some acceptable subspace. However, in absence of space we shall skip this step.

By this method the α_b of equation (2) are determined from the sensor outputs.

For the sake of generality we define the sensor output s_k at point k to be a function f_k of a linear combination of the strains at all nodes i, weighted by coefficients a_{kui} according to the expression

$$s_k = f_k(a_{kui}e_{ui}) \quad \text{for} \quad (k \in \{1, \ldots, q\}), \tag{3}$$

where q represents the number of sensors used.

This expression captures both nonlinear and linear sensor model behavior. It is obvious here that the coefficients a_{kui} may play the role of switching on and off the influence of strain components at surrounding nodes, from all to none. Figure 2 shows the sensor output space relative to the geometry of the structure. In this figure the vertical lines signify the amplitude of the sensor output and the small lines on the plane indicate the sensor direction. This provides freedom in orienting the sensors. We emphasize here that the sensor location need not be at a nodal point. Expression (3) allows interpolation from the surrounding nodal points.

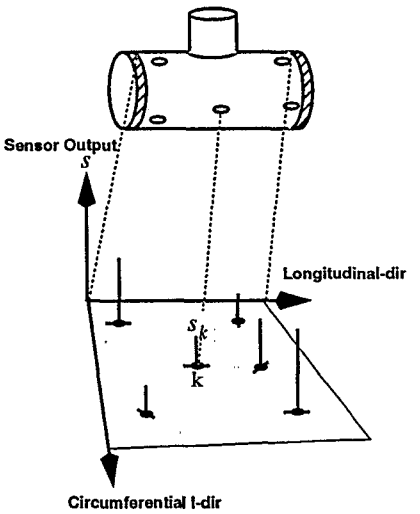

Fig. 2. Sensor output space associated with the geometry of the structure.

An example of such a model is the Extrinsic Fabry-Perot Interferometer (EFPI) optical fiber sensor with a transfer function given by [3]

$$\Delta\phi_k = \frac{4\pi\Delta\lambda}{\lambda_1\lambda_2 L}e_k, \tag{4}$$

where the coefficients a_{kui} are functions of the light sources used (λ_1, λ_2 are the wavelengths of the laser sources used) and geometrical properties of the sensor (L is the gage length of the EFPI sensor). In the optical fiber case it is always assumed that only the local strain components are going to affect them. The role of the sensor output is played by the fringe count difference $\Delta\phi_k$. In general the coefficients a_{kui} not only reflect influence of the neighborhood, but also contain calibration information for the sensors. The effect of embedding sensors into a material must be determined experimentally. This can be done by weighting the known transfer function of a sensor for the non-embedded case (as in expression (4)), so that the predicted strains will agree with the values measured from an independent and known source such as sets of strain gauges.

Computing strains from sensor outputs requires the inverse g_k, ($g_k = f_k^{-1}$), of the sensor transfer function. Composing both sides of equation (3) with the inverse function f_k^{-1} yields to:

$$f_k^{-1}(s_k) = f_k^{-1}(f_k(a_{kui}e_{ui})), \tag{5}$$

or

$$g_k(s_k) = a_{kui}e_{ui}. \tag{6}$$

Introducing equation (3) into equation (6), we obtain the inverse transfer function depending only on the basis loading case strain fields, i.e.

$$g_k(s_k) = a_{kui}e_{ui}(L_b)\,\alpha_b. \tag{7}$$

Provided the pseudo inverse matrix $[a^{kui}e^{b}_{ui}]^P$ exists, the coefficients α_b can be determined uniquely from (7) according to the equation

$$\alpha_b = [a_{kui}e_{ui}(L_b)]^P g_k(s_k). \tag{8}$$

We can now compute the predicted nodal strains e'_{ui} by introducing equation (8) into equation (2):

$$e'_{ui} = e_{ui}(L_b)\,[a_{kui}e_{ui}(L_b)]^P g_k(s_k). \tag{9}$$

The necessary and sufficient conditions for the existence of the pseudoinverse array

$$t_{kb} = [a_{kui}e_{ui}(L_b)]^P, \tag{10}$$

is that the number of basis loading cases r be equal to or less than the total number of sensors q i.e.

$$r \le q, \tag{11}$$

and that the array $a_{kui}e_{ui}(L_b)$ is non-singular.

To address the problem of using finite computational resources for very high dimensional loading spaces, one employs the approach of utilizing apriori knowledge about the temporal character of loading conditions, to involve lower dimensioned loading subspaces for finite durations.

2.2. Material Health from Dissipated Energy Density

For the last 20 years NRL has been developing an approach to characterize strain induced material damage [1]. This approach was motivated by a need to model failure behavior in composites on a continuum basis and of relating it to material constitutive behavior. The goal of such an approach is to permit accurate modeling of the progressive loss of stiffness and concomitant inelastic behavior.

The procedure involves the determination of an *energy density dissipation function* ϕ that only depends on the strain vector $\underset{\sim}{\varepsilon}$ and the material used in the structure, according to:

$$\phi(\underset{\sim}{\varepsilon}, m) = \phi(\underset{\sim}{\varepsilon}, \underset{\sim}{c}) = c_1(m)\chi_1(\underset{\sim}{\varepsilon}) + \ldots + c_m(m)\chi_n(\underset{\sim}{\varepsilon}) = c_i(m)\chi_i(\underset{\sim}{\varepsilon}), \tag{12}$$

where, $\underset{\sim}{c}$ represents the vector of the material depended coefficients c_i, and χ_i represents the basis functions depending only on strains $\underset{\sim}{\varepsilon}$ and defined at a total of n distinct points distributed over the strain space. Equation (12) can be thought as being an interpolation function allowing evaluation of ϕ on points other than the ones used to define the basis functions.

Its volume integral equals the energy dissipated during loading due to the various internal failure events, and its value at any point in the material is regarded as a measure of load induced internal damage. The energy dissipation function is connected through the total energy offered into the system when loaded and the recoverable energy, through the relationship:

$$\int_0^{u_r} t_u q_v dq^v - \frac{1}{2} t_s u_t u^v = \int_{\partial V} \phi(\varepsilon_i(x_j))\,dx_j \tag{13}$$

The energy density dissipation function thus captures the collective behavior of these failure mechanisms without requiring an explicit knowledge of these mechanisms, and, moreover, can also be related to local stiffness changes which characterize nonlinear structural behavior. The left hand side of equation (13) is known through the automated experimental procedure that involves the In-Plane-Loader (a three degree of freedom robotic testing machine) [1,2].

Close similarities between acoustic wave attenuation distributions of damaged specimens with the corresponding predicted distributions of dissipated energy density as they are shown in figure 3 for three different loading paths, furthermore enhance the connection of the dissipated energy density with the internally created micro damage.

The energy density dissipation function is determined from an extensive set of test data obtained from NRL's In-Plane Loader [2]. This is a computer controlled testing machine capable of producing multiple combinations of opening/closing, sliding, and rotating boundary displacements.

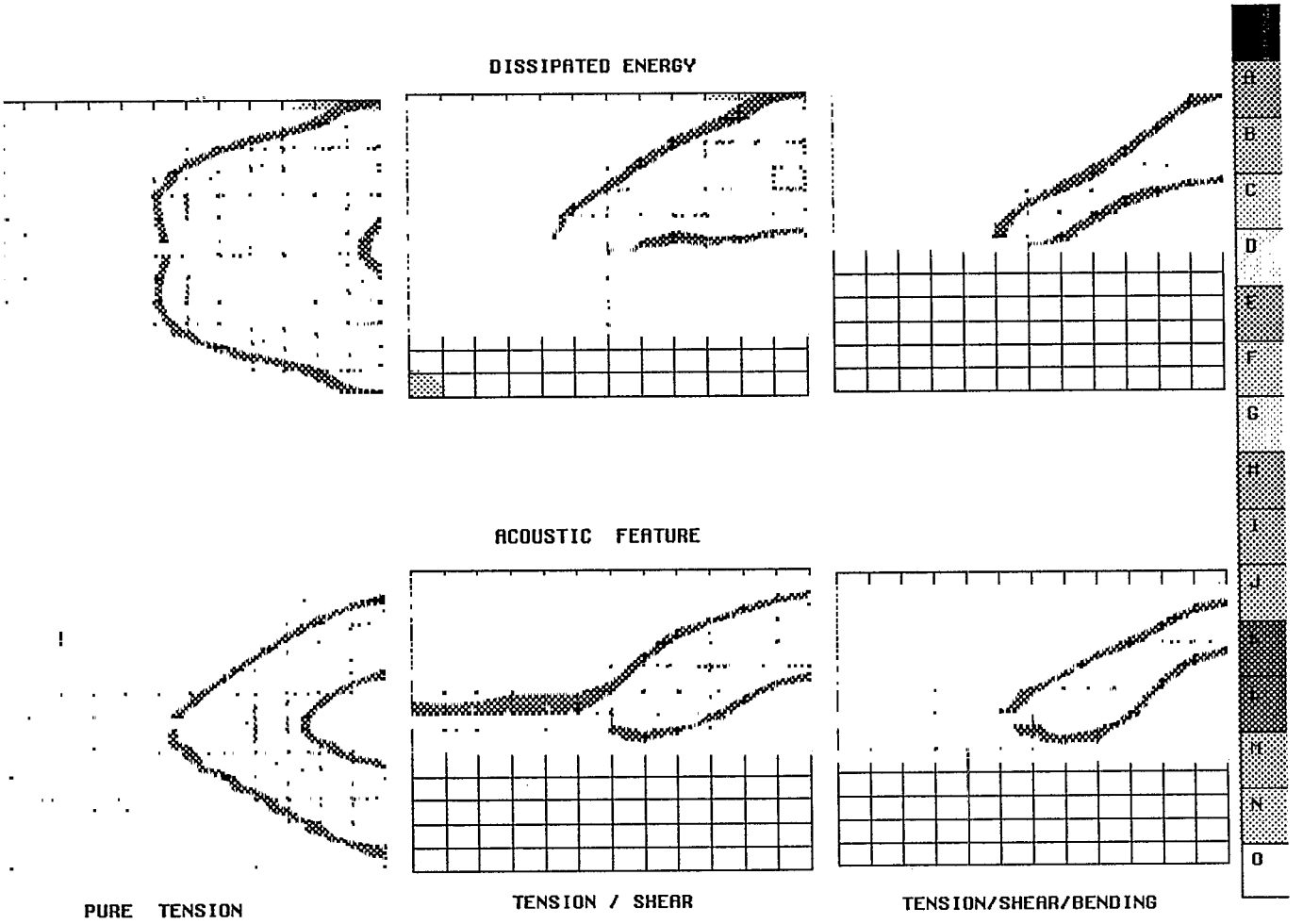

Fig. 3. Dissipated energy density distributions (top row) compared to acoustic attenuation (bottom row) for three different types of loading of a notched specimen.

In the recent years the dissipated energy density function has been used by NRL not only as a measure of local material softening due to load induced damage, but also as a quantity to describe the non-linear damage response of composite materials as well as the global softening response of composite structures.

It is therefore, very natural to consider that since the dissipated energy density effectively provides a measure of damage, that the health of the material can be expressed at any point in the structure as a complementary quantity. One can view a situation, in which the observer of a dissipated energy density contour map on a structure, associates good health of the material at places of low dissipated energy density.

The dissipated energy density at every point in the structure can be computed if the strains are known. Computing and plotting the dissipated energy density contour or fringe maps over the entire structure thus becomes a computationally intensive though trivial task.

In the context of the present paper the dissipated energy density can be plotted for the actual strains as computed from the forward analysis for a given loading condition and then from the sensor predicted strains as they are obtained from equation (9). Theoretically if condition (11) is satisfied the comparison between these two maps should show no difference. However, in the case of controlled conditions, a variation between the two images may indicate the need for fine tuning of the calibration coefficients for the selected sensor network. It can also be used to select an alternative sensor system and establish its corresponding calibration in-situ.

2.3. Embedded Sensors for Smart Structures Simulator

To facilitate the process of displaying the dissipated energy density maps in a dynamic fashion, and for a variety of parameters that may be dynamically varied by the user, NRL has initiated the development of the ES[4] system. This system has been designed to assist the user in satisfying the objectives described in the introduction.

The components of the simulator and their function can be described as follows.

- *Structural System Simulator:* Allows definition of geometry, material and loading events and computes strains induced in composite structures from operational loads.
- *Dissipated Energy Simulator:* Computes dissipated energy density from strains.
- *Sensor Simulator:* Allows specification of the sensor network parameters and computes sensor output from strains for various sensor types.
- *Strain Predictor:* For a particular sensor placement, computes strains at any location from sensor outputs.
- *Criteria:* Computes a satisfaction value for a specific sensor placement and provides feedback to the sensor and structural simulators. The satisfaction value can be provided manually by the user or automatically evaluated from an apprentice mechanism that makes use of previous interactions between users and simulator.

Figure 4 shows the block diagram of the simulator with the functional dependence of the modules represented from the data flow arrows between the blocks.

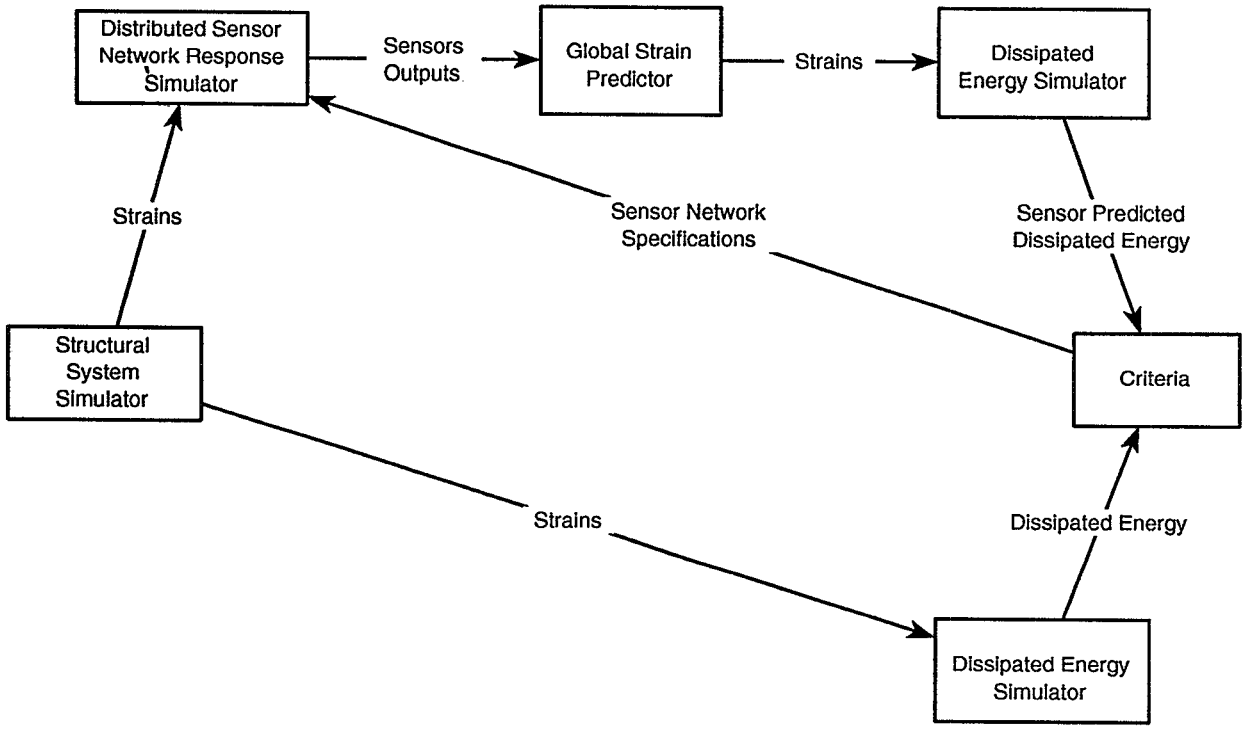

Fig. 4. Data flow block diagram of the ES[4].

At present the structural system simulator and the dissipated energy simulator are the furthest advanced. The sensor simulator and the strain predictor still need optimization, while the criteria module has only been defined. The software involved includes both commercial and custom packages, and is currently running in a distributed fashion over NRL's network of NeXT and SGI workstations and a CRAY YMP/EL. There are plans for developing a single workstation version of the simulator.

3. CASE STUDY AND RESULTS

The selected geometry consists of two orthogonally intersecting cylinders as shown in Figure 5. The smaller cylinder is of an AS4/PEEK (+/- 60) laminated composite thermoplastic material with an elliptic cross section and has a top of the same material, while the larger cylinder is of an AS4/3501-6 25(0)/67(+/-45)/8(90) laminated composite thermoset material with a circular cross section and has two steel end caps.

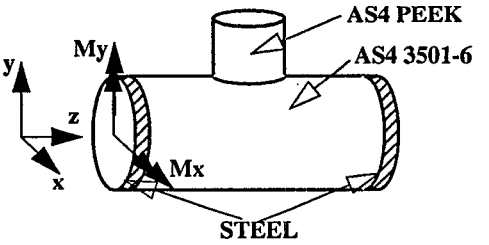

Fig. 5. Geometry, material and loading specification for intersecting cylinders model.

Three basis loading cases were selected. External hydrostatic pressure to capture the effect of depth, and bending about the x-axis and y-axis respectively, in order to capture underwater explosion and maneuvering events. Combinations of these three cases represent a large class of actual loading events. Figure 6 shows the loading space and load vectors that represent potential loading paths. Because of the y-z plane symmetry of the structure only half of the loading space needs to be considered.

The labels for the loading cases in figure 6 have been chosen to indicate the participation of the three basis cases with "+" or "-" depending on the sense, and the absence with "0". The first position on the label represents the pressure loading case, the second and the third represent the bending loading about the x- and y-axes respectively.Finite element discretization was applied to this model by utilizing the structural simulator module. Shell elements were used and the structural analysis results for the three basis cases obtained. The moment loading conditions were applied by unit pairs of forces on the steel end cups. And the results for the combined loading cases were obtained by using relation (4).

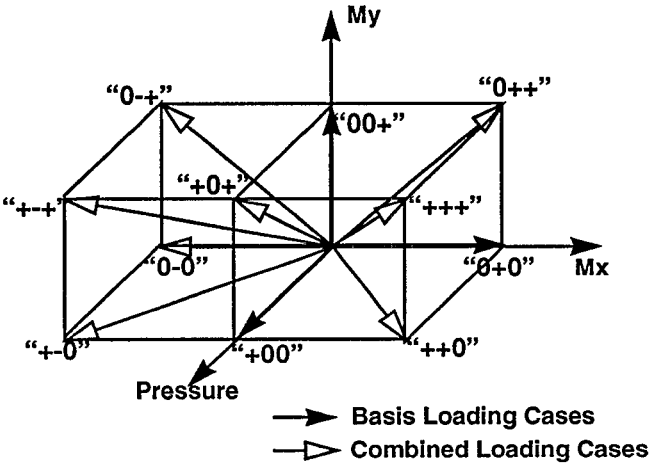

Fig. 6. Basis and combined loading paths embedded in the loading space.

In figure 7(a) the fringe plot of dissipated energy density over the deformed structure is shown for the 5th increment of combined loading case "+++". This image is one of the frames that the dissipated energy density simulator can produce when presented with the strain fields on the structure. To the extent that the actual and sensor predicted strains are the same, the corresponding dissipated energy density maps should be identical such as in figure 7(a), because dissipated energy density is solely a function of strains.

A scheme was developed to describe the effects of sensor incapacitation in the case of redundant sensors, even though it will not be presented.

The curves in figure 7(b) represent the evolution of the total dissipated energy in the structure as a function of load increments for the three basis cases and for the combined case in which all basis cases participate. The total dissipated energy is computed by integrating the dissipated energy density over the volume of the structure. This quantity can be used as a measure of the global structural loss of stiffness or the global softening of the structure. Depending on the boundary conditions this curve can also represent the evolution of load drop due to total accumulated damage. The two bending basis cases "0+0" and "00+" look alike. In the region between the 4th and the 6th load increments they exhibit a difference due to the fact that the second elliptical cylinder exhibits a stiffer behavior for the case "00+". The hydrostatic pressure loading case "+00" presents a substantially stiffer behavior for the loading steps higher than 4. As expected the combined case presents the worst in that it exhibits the highest rate of softening.

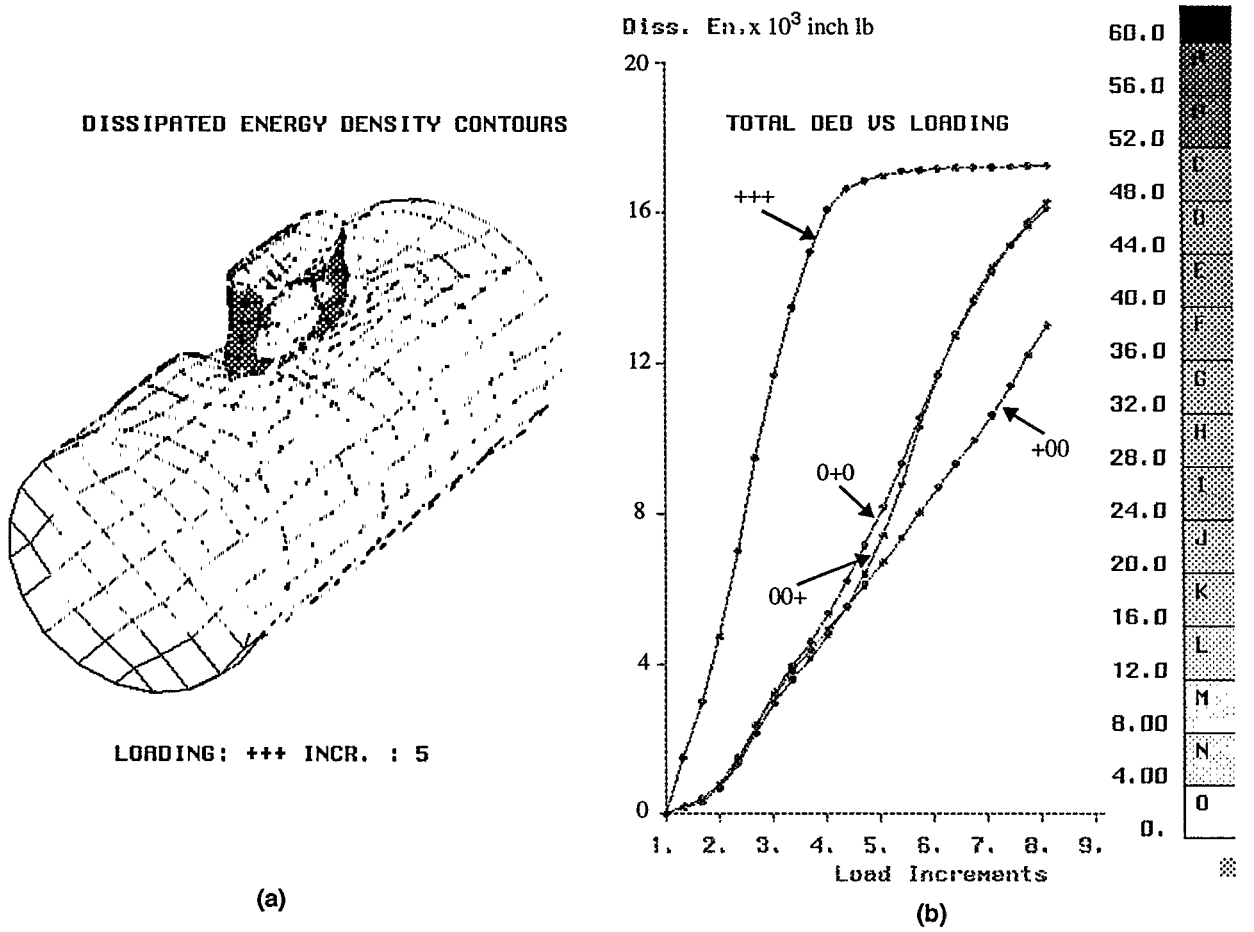

Fig. 7. Dissipated energy density distribution (a) and variation of total dissipated energy vs. load increments for various loading cases (b)

4. DISCUSSION AND CONCLUSIONS

Sensor Network Selection:
The proposed methodology facilitates the selecting of appropriate sensor types and in their number and placement.

Selecting the kind of needed sensors can be a function of many issues that the designer may wish to address. Certain non-mechanical requirements may prevail (i.e. crosstalk, electromagnetic interference isolation) that may narrow down candidate sensors to one or two families. Mechanical requirements like embeddability may be used to further narrow the selection. This approach can aid the designer in making decisions about sensor sensitivity and dynamic range.

Selecting the number of required sensors can also be facilitated by our approach. Since it has been established by equation 11 that the number of required sensors has to be at least as large as the number of the expected loading basis cases, the problem has been reduced to deciding the degree of redundancy needed for a specified fault tolerance. A redundant sensor system can be implemented to allow strain prediction recovery in case of sensor fault, partial or total sensor incapacitation. The sensor simulator module provides the designer with the capability of performing "what-if" studies of prediction deterioration as a function of varying degrees of redundancy and varying degrees of sensor incapacitation.

The coefficients a_{kui} carry the following type of information:
- sensor constants (i.e. optical, material, electrical, thermal properties),
- effects of the non local behavior of the sensor or the sensor network. (i.e. a sensor can be affected from strains in neighboring areas, or a sensor output depends an the triangularization from surrounding points)

embeddability and material system compatibility effects (i.e. combined response of the sensor when embedded in the material, and effects of

ingress/regress areas to the sensing area, and effects of other material constituents such as actuating devices).

The sensor simulator module provides a capability for describing any sensor transfer function, with emphasis on allowing continuous variation of these parameters. This can help the potential designer in allowing "what-if" studies to address these issues.

Sensor Network Calibration:
Performing sensor network calibration may now be greatly enhanced by virtue of the fact that with appropriate simple experiments the coefficients a_{kui} can be determined in a way which accounts for all of the effects mentioned above, and without specific knowledge of the micro-mechanical effects. This is done by requiring the sensor detected strains be as close as possible to the actual ones.

Loading Events Simulation:
Through the linear elastic analyses that associate the basis loading cases with the basis strain cases and relations (2) and (9) the loading condition can be reconstructed from the sensor output. Plans exist to extend the structural simulator so as to include a loading event module that can be set to display in terms of actual independent loading events (i.e. underwater depth variation, or depth charge parameter variation).

Prediction of material/structural health depends on the determination of a of a function that maps the dissipated energy density distribution of the smart structure, to the value space of those empowered to say when the structure is or isn't performing its task. We do not pretend to offer this function; only potentially an environment in which it may be determined (i.e. a concept formation laboratory).

5. ACKNOWLEDGMENTS

The authors would like to gratefully acknowledge the financial support provided by ARPA under contract no. 6604. We would also like to express our gratitude to Mr. James Kelly for his encouragement and support.

6. REFERENCES

1. P.W. Mast, G.E. Nash, J.G. Michopoulos, R.W. Thomas, R. Badaliance, and I. Wolock, "Experimental determination of dissipated energy density as a measure of strain-induced damage in composites", Technical Report NRL/FR/6383--92-9369, Naval Research Laboratory, Washington, DC.,1992.

2. P.W. Mast, L.A. Beaubien, M. Clifford, D.R. Mulville, S.A Sutton., R. Thomas, J. Tirosh, and I. Wolock, "A semi-automated in-plane loader for material testing", *Experimental Mechanics*, Vol. 32, pp. 236-241,1983.

3. Claus, R.O., Gunthor, M.F., Wang, A., and Murphy, K.A., "Extrinsic Fabry-Perot sensor for strain and crack opening displacement measurements from -200 to 900 °C", *Smart Materials and Structures*, Vol. 1, pp. 237-242, 1992.

E-mail Inquiries:
Technical: JGM: yiannis@prologos.navy.mil, PWM: mast@tao-too.nrl.navy.mil
Programmatic: RB: bob@bozo1.nrl.navy.mil, HC: henry@ch.nrl.navy.mil